

Living with a Red Dwarf: The Rotation–Age Relationships of M Dwarfs

SCOTT G. ENGLE¹ AND EDWARD F. GUINAN¹

¹*Villanova University*

Dept. of Astrophysics and Planetary Science

800 E. Lancaster Ave

Villanova, PA 19085, USA

ABSTRACT

Age is a fundamental stellar property, yet for many stars it is difficult to reliably determine. For M dwarfs it has been notoriously so. Due to their lower masses, core hydrogen fusion proceeds at a much slower rate in M dwarfs than it does in more massive stars like the Sun. As a consequence, more customary age determination methods (e.g. isochrones and asteroseismology) are unreliable for M dwarfs. As these methods are unavailable, many have searched for reliable alternatives. M dwarfs comprise the overwhelming majority of the nearby stellar inventory, which makes the determination of their fundamental parameters even more important. Further, an ever-increasing number of exoplanets are being found to orbit M dwarfs and recent studies have suggested they may have a relatively higher number of low-mass planets than other spectral types. Determining the ages of M dwarfs then allows us to better study any hosted exoplanets, as well. Fortunately, M dwarfs possess magnetic activity and stellar winds like other cool dwarf stars. This causes them to undergo the spindown effect (rotate with longer periods) as they age. For this reason, stellar rotation rate has been considered a potentially powerful age determination parameter for over 50 years. Calibrating reliable age-rotation relationships for M dwarfs has been a lengthy process, but here we present the age-rotation relationships for \sim M0–6.5 dwarfs, determined as part of the *Living*

with a Red Dwarf program. These relationships should prove invaluable for a wide range of stellar astrophysics and exoplanetary science applications.

Keywords: Stellar ages (1581); Stellar rotation (1629); Low mass stars (2050); Photometry (1234); Late-type dwarf stars (906); M dwarf stars (982); White dwarf stars (1799)

1. INTRODUCTION & BACKGROUND: STUDYING M DWARFS

Main sequence (dwarf) M stars (dM stars; red dwarfs; referred to as *M dwarfs* hereafter) represent the cool, low mass, low luminosity end of the main sequence, and comprise $\sim 75\%$ of all stars in the solar neighborhood (Reyl e et al. 2021). This study specifically focuses on M0 V – \sim M6.5 V stars, with properties ranging from: Mass $\approx 0.6 - 0.1 M_{\odot}$; Radius $\approx 0.6 - 0.1 R_{\odot}$; Luminosity $\approx 0.06 - 0.001 L_{\odot}$ and temperatures $T_{\text{eff}} = 3900 - 2850 \text{ K}^1$.

M dwarfs have received substantial attention during the 2000’s, prompted in part by the discovery that these numerous stars host a relatively large number of terrestrial-size planets (Rojas-Ayala 2023; France et al. 2020; Hsu et al. 2020) when compared to stars of higher mass. Aside from the large number of nearby M dwarfs available for study, they also make very attractive targets for terrestrial planet searches and research programs as such planets are more readily detected through radial velocity motions and planetary transits due to the low masses and small radii of the M dwarf host stars. Estimates of the frequency of potentially habitable planets (PHP) hosted by M dwarfs have been made primarily from *Kepler* Mission data, but also from numerous radial velocity studies. Conservative estimates place the planetary frequency around 15% (Dressing & Charbonneau 2013) and studies including expanded circumstellar Habitable Zone (HZ) estimates indicate higher frequencies of $\sim 30\text{--}40\%$ (Hsu et al. 2020; Kopparapu 2013). If a slightly conservative ‘middle ground’ of 25% is adopted, it implies that within 10 pc (~ 33 ly) of the Sun (a volume of space containing ~ 240 M dwarfs), there should be ~ 60 potentially habitable Earth-size planets. Extrapolating to include

¹ https://www.pas.rochester.edu/~emamajek/EEM_dwarf_UBVIJHK_colors_Teff.txt

the entire Milky Way raises the possibility that billions of Earth-size planets are orbiting within the habitable zones of M dwarfs.

M dwarfs are equally fascinating targets for stellar astrophysics. Relative to their sizes, they display enhanced magnetic dynamo activity due to the extent of their interior convective zones. As a result, their coronal and chromospheric emissions are also relatively strong, compared to their bolometric luminosities. They have comparatively slow core nuclear reaction rates, however, which makes them rather ‘fuel efficient’ and results in their long main-sequence lifetimes. More massive M dwarfs can live on the main sequence for over 100 Gyr while those of lower mass ($M < 0.2 M_{\odot}$) can live as long as ~ 1 trillion ($\sim 10^{12}$) years (Choi et al. 2016). Due to this, no M dwarfs have yet to evolve off the main sequence. Another consequence of their long lifetimes, however, is that once M dwarfs reach the core hydrogen-fusing main-sequence their basic physical properties (L , T_{eff} , R) remain essentially constant over cosmological time scales (i.e., ~ 14 Gyr).

Their large numbers, longevities, and near-constant main sequence luminosities make M dwarfs very compelling targets for programs searching for life in the universe since, unlike our Sun, the HZs and thus exoplanet bolometric irradiances (and planetary instellations) remain stable for tens of Gyrs or longer. However, the stars’ very slow nuclear evolution makes determining accurate stellar ages extremely challenging (see Soderblom 2010, and references therein).

Fortunately, it has been known for 50 years (Skumanich 1972) that cool dwarfs undergo a ‘spindown effect’ whereby their rotation periods lengthen as they age. Since that time, numerous studies have shown the potential that stellar rotation holds as an age determinant – the method known as “gyrochronology” (Barnes 2003, 2007; Mamajek & Hillenbrand 2008; Engle & Guinan 2011, 2018; Pass et al. 2022). Late-F, G, K, and M dwarfs have stellar winds and magnetic fields which act in tandem to propagate the spin down effect. The winds of these stars are magnetically-threaded, continually carrying small amounts of each star’s mass out into space while it is still (over a certain distance) tethered to the star itself by the magnetic field. The mass eventually escapes the magnetic field entirely, but its magnetically-threaded tenure has already caused a slowing of the star’s rotation due to conservation of angular momentum (Kawaler 1988).

This spindown effect allows magnetic activity levels (observed through such proxies as X-ray and UV [X–UV] emissions, and several emission features known to exist within optical spectra) to serve as additional age determinants for cool dwarfs. Activity-age relationships have been also been constructed for M dwarfs, and they will be detailed in a follow-up paper.

The largest difficulty resided in building a representative sample of M dwarfs with a wide range of previously known ages and then determining their rotation periods. In this paper we present these ‘benchmark’ objects and the rotation-age relationships of M dwarfs determined as part of the *Living with a Red Dwarf (LivRed)* Program.

2. DATING M DWARFS: DETERMINING AGES FOR (MOSTLY) AGELESS STARS

Age, along with mass and composition, is one of three key factors governing a star’s current state [Soderblom \(2010\)](#), yet it is also one of the most difficult stellar parameters to accurately measure. As mentioned, this is particularly true with M dwarfs, for which other commonly applied methods (e.g., isochronal, asteroseismic) for aging a star are unreliable [Lu et al. \(2021\)](#). Observables, such as rotation period and X-UV activity level, are known to be age-dependent and are often related to each other, but relating either quantity to stellar age first requires a set of M dwarfs with known ages – a benchmark sample.

With no currently available methods for directly determining the ages of single, isolated M dwarfs, the sample of benchmark M dwarfs has instead been built using *age by association*. Each benchmark either has a stellar companion or belongs to a larger group or population of stars within the galaxy. For each pairing or grouping of stars, it is the age of the companion star or the group that can also be applied to the M dwarf since they are assumed to have formed at the same time.

The age by association method in this study can be divided into three categories. For young dwarfs with ages below ~ 2 Gyr there are several well-studied ‘stellar groups’ (referred to as either moving groups, clusters, or associations) available. The ages are very reliable, but sadly do not cover nearly the range that we need. There are a limited number of additional clusters with greater ages, but other issues exist. For example, in the clusters NGC 752, and Ruprecht 147 (ages of 1.4, 2.5, and 2.7 Gyr – see [Gruner & Barnes 2020](#); [Curtis et al. 2020](#), and references therein) rotations periods

have only been measured for earlier M dwarfs. A small number of HR 1614 moving group members (age ~ 2.0 Gyr – [60]) with rotation periods were once used, but the coherence of the moving group itself has recently been called into question [Kushniruk et al. \(2020\)](#) which prompted their removal as benchmarks. Traditionally, the distances of highly prized targets such as M67 and NGC 188 (ages 4 Gyr) prevented sufficient time-series photometry any their faint M dwarf members. However, [Dungee et al. \(2022\)](#) have recently measured rotation rates within this cluster for stars as late as $\sim M3$, showing some of the exciting recent progress in cluster gyrochronology measures.

Ages can also be assigned to stars that are members of specific galactic populations. Additional benchmarks were selected which belong to either the Thick Disk or Halo populations (ages of ~ 8 –11 and ~ 10 –12.5 Gyr) of the Milky Way, based primarily on the star’s *UVW* galactic space motions ([Leggett et al. 1998](#); [Bensby et al. 2014](#)), with further support of membership from metallicity values and velocity dispersions ([Yu & Liu 2018](#)). The advanced ages of these populations make them important benchmarks, but more direct age estimates for individual M dwarfs, as opposed to statistically-supported, kinematically-inferred ages, would usually be preferred.

The final and very welcome source of benchmarks is M dwarfs that belong to common proper motion (CPM) pairs/systems with an age-determinable companion. If the companion is a more massive (F–G dwarf) star, then a reliable age can be determined by other, more common (e.g., isochronal and/or asteroseismic) methods and applied to the (assumed to be coeval) M dwarf. Systems with white dwarf (WD) companions have become increasingly useful due to advances in determining the WD progenitor star properties (see [Cummings et al. 2018](#)) that have resulted in increasingly reliable ages. It is always important to note that the separation of the M dwarf from its companion is assumed to have prevented past interactions, allowing the M dwarf to evolve as if it were a single, isolated star. Though, for specific pairs (particularly those with small separations is small), the possibility of past interactions may exist (see [Pass et al. 2022](#)). However, a particular benefit these systems have over the previously mentioned CPM pairs is that the WDs do not outshine their M dwarf companions, which facilitates CCD photometry of the M dwarfs to search for rotation periods. These systems provided several M dwarf targets with ages older than 2 Gyr: an age-range that was long-awaited

additional targets. Determining rotation periods for these older M dwarfs became a primary focus of the program.

For this study, multiple (if available) measures of each WD companion’s effective temperature (T_{eff}) and surface gravity ($\log g$) were gathered from the recent literature, and mean values and uncertainties were determined via χ^2 analysis. With these values, updated ages and uncertainties were calculated using both the `WD_Models` package, written by Dr. Sihao Cheng, and the `wdwarfdate` package, written by Dr. Rocio Kiman (Kiman et al. 2022). Both incorporate the latest WD cooling models available Bédard et al. (2020) and the initial-final mass relationship (IFMR) of Cummings et al. (2018). We note that this is not the only IFMR choice available within the `wdwarfdate` package, but it is the one we selected for consistency with `WD_Models`.

3. STARING AT M DWARFS: DETERMINING ROTATION PERIODS

The surface features (e.g. starspots) of cool, main sequence stars will be brought in and out of view as the stars rotate, if the orientation of the star (inclination of the star’s rotation axis relative to our line sight) and the star spot surface distribution are favorable. Repeatedly measuring stellar brightness via photometry can determine the rotation periods by revealing cyclical changes in brightness over time. This was the preferred method for determining benchmark rotation periods, as it is precise and works for very long rotation periods where spectroscopic measures of rotation velocity become ambiguous. Measuring rotation via photometry is a very straightforward process on paper, but in practice substantial difficulties can arise when dealing with M dwarfs. As the *Living with a Red Dwarf* program was designed to study the crucial missing age-range of >3 Gyr, it was unknown at the outset, but this would mean measuring rotation periods anywhere from ~ 30 days to as long as ~ 150 – 170 days. Such extended rotation periods require rather lengthy observing campaigns. As light amplitudes can be below ~ 0.015 mag, the photometry requires a sufficiently high precision as well. Further, successfully detecting a rotation signal depends on the star maintaining a ‘favorable’ (non-uniform) distribution of starspots, possibly for several years. Fortunately, many of the M dwarfs observed in this program have displayed a persistence of surface features – in some cases for several

years. Though most of our targets are significantly older, our results thus far align with those of [Robertson et al. \(2020\)](#), which studied 4 young, rapidly rotating M dwarfs.

Apart from cluster members, whose rotation periods were obtained from the literature (see Tables 1 and 2), the vast majority of benchmark rotation periods were determined through dedicated CCD photometry of the targets carried out with the 1.3 meter *Robotically Controlled Telescope (RCT)* – [Strolger et al. 2014](#)) at *Kitt Peak National Observatory* in Arizona. In limited cases, data (or additional data) were obtained using other telescopes (e.g., the 0.8 meter *Automated Photoelectric Telescope (APT)* – see [Engle 2015](#)) or publicly available surveys, either due to target visibility or to help confirm the rotation period. Except for the faintest sources, photometry was carried out in the *V*-band, with *individual* measurement uncertainties of typically ~ 0.004 – 0.01 mag depending on the brightness of the star. Data would be removed prior to analysis for reasons ranging from legitimate hardware malfunctions, to poor sky quality conditions, even down to a large moth having taken a poorly timed stroll through the telescope’s light path. For *RCT* / *APT* targets, 3 – 5 measures were obtained per night, from which nightly means and uncertainties were determined. The yearly and multi-year data sets were searched for periodic variations with the Generalized Lomb-Scargle and CLEANest algorithms, (as implemented within *astropy* ([Astropy Collaboration et al. 2013, 2018, 2022](#)) and *Peranso* (v3) ([Paunzen & Vanmunster 2016](#))) an example of which is shown in Fig. 1. All rotation signals have false alarm probabilities below 1%.

In limited cases, additional or alternative sources of photometry were used to determine rotation periods. Proxima Cen and Kapteyn’s Star have been a part of the program for several years, but are southern hemisphere targets and thus inaccessible to the *RCT*. Observing time on the Skynet Robotic Telescope Network was purchased, and CCD photometry was carried out using the network’s *PROMPT* telescopes at the *Cerro Tololo Inter-American Observatory* in Chile and the *Meckering Observatory* in Australia. Images were automatically reduced before downloading, and nightly means were determined and analyzed in similar fashion to *RCT* / *APT* data.

The remaining cases consist of targets that were added to the program only recently. Due to the installation and testing of a new and upgraded camera system, and the Contreras wildfire, the

RCT experienced an observing hiatus. With a good combination of photometric depth, precision, and timeline, *Zwicky Transient Facility* data were used as an alternative. Individual measures were downloaded from the *NASA/IPAC* Data Archive, excluding any measures the archive had flagged. The resulting data were then sigma-clipped (also within *astropy*) before nightly means were constructed.

Rotational light curves of the benchmark M dwarfs are shown in Fig. 2 to give an idea of the amplitudes of variability observed and of the data quality. M dwarf rotation amplitudes can range from ~ 0.01 mag or less in the “toughest” cases to as much as 0.06 mag for ideal cases such as Proxima Cen.

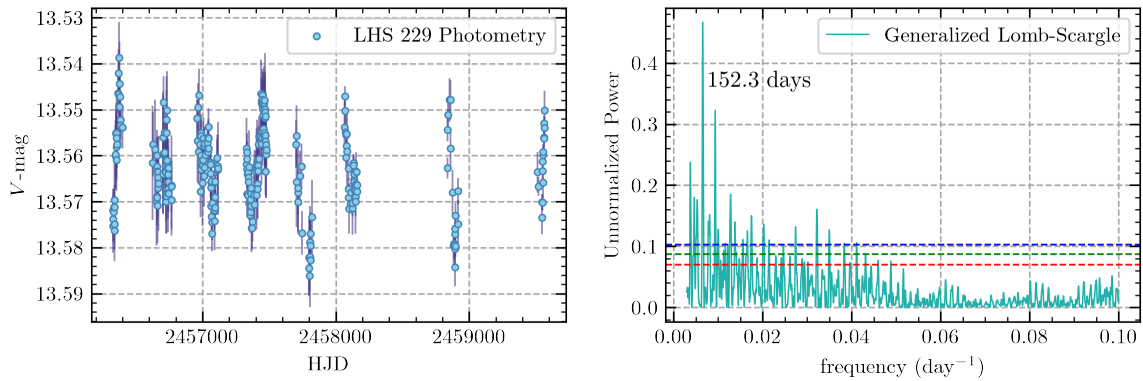


Figure 1. An example lightcurve for one of our mid-late benchmark stars, LHS 229, whose age of ~ 8.7 Gyr (see Table 2) was determined from its WD companion, LHS 230 (see Table 3). At left, the full time-series dataset is plotted, covering a span of 10 years. At right, the Generalized Lomb-Scargle periodogram (via *astropy*) results are plotted, in frequency-space, and the dashed, horizontal lines indicate false alarm probabilities (FAPs) of 10% (red), 1% (green), and 0.1% (blue). A rotation period of ~ 152.3 days was found, and the phased lightcurve is plotted in Fig. 3.

4. 4. RESULTS & DISCUSSION – A TALE OF TWO RELATIONSHIPS

The primary focus of the *Living with a Red Dwarf (LivRed)* program has been to characterize the evolution of M dwarf rotation rates over their lifetimes, with the end goal of providing a reliable method for calculating the age of an M dwarf, so long as its rotation period has been determined. When comparing related, age-associated quantities (e.g., activity and rotation) the data is commonly

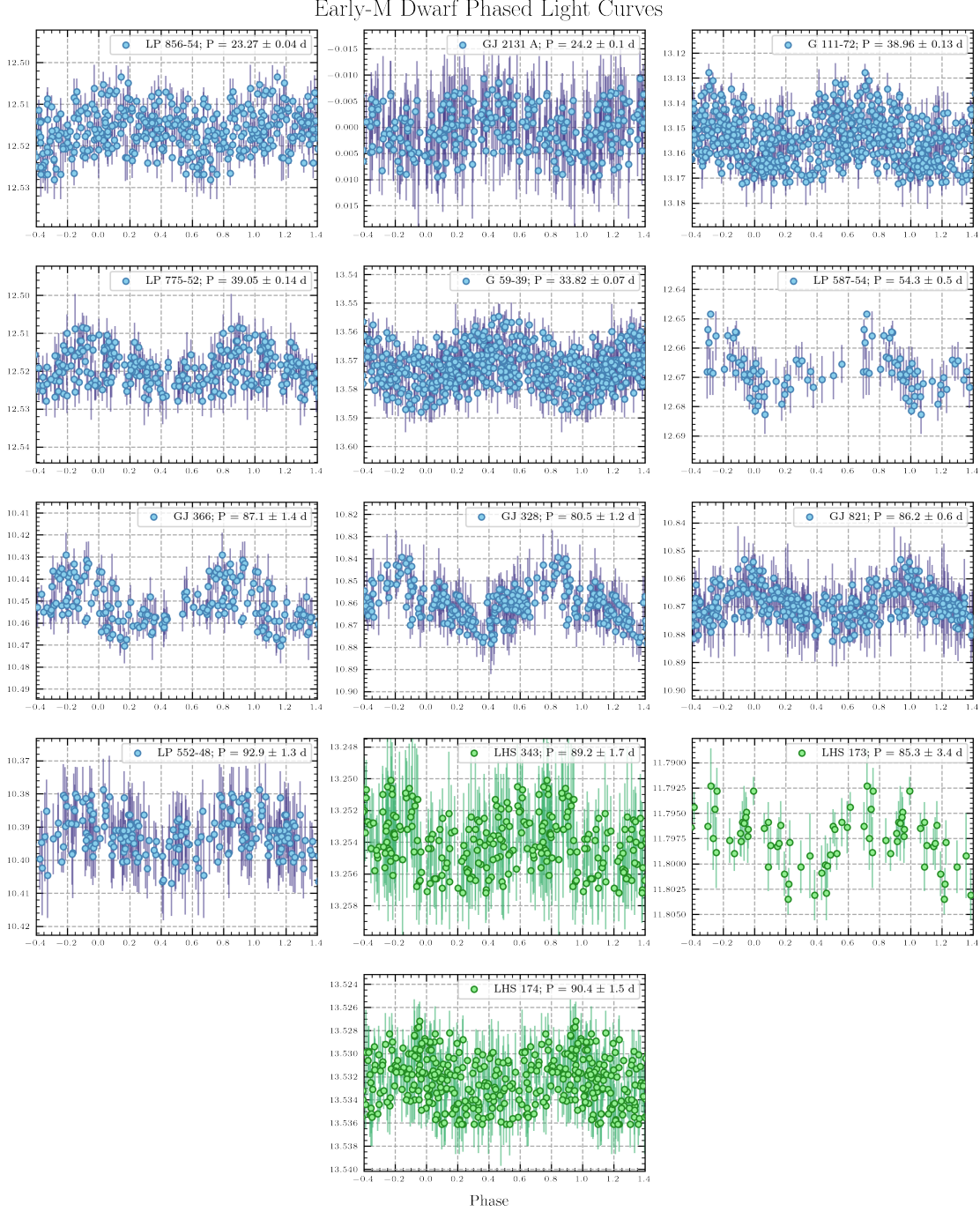


Figure 2. The phased rotation light curves of the early M dwarf benchmarks. The name and rotation period (and uncertainty) of each star is inset within their respective plot. The ‘scatter’ of the data along the y-axis is primarily due to variations in lightcurve shape and amplitude over the different observing seasons. For plots where the magnitudes are centered on zero, either a long-term trend or cycle was first removed from the data prior to conducting the rotation period search. Data are color-coded according to their source: blue for data that we acquired with the *RCT* (and *APT* in limited cases), green for public *ZTF* data (IRSA 2022), and beige for data we obtained with the *Skynet* telescope network.

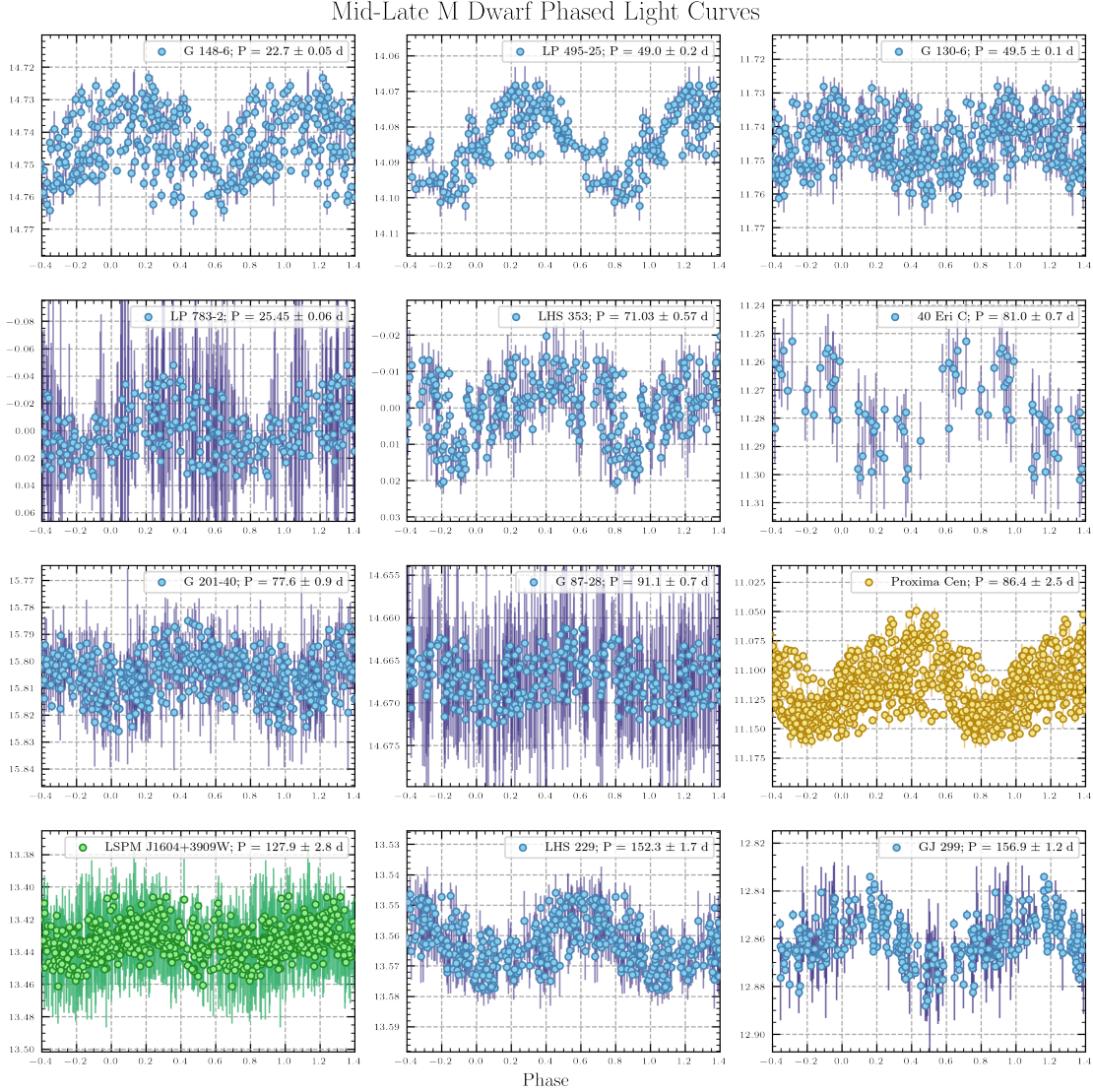


Figure 3. The phased rotation light curves of the mid-late M dwarf benchmarks (additional lightcurves are plotted in Fig. 4). The data coloring scheme from Fig. 2 is applied here and, again as in Fig. 2, a plot where magnitudes are centered on zero indicates that a long-term trend or cycle has been removed.

linearized by taking the logarithms of both quantities. In our analysis of M dwarf age vs rotation, we found that both subsets of M dwarfs (but particularly the mid-late subset) showed deviations from linearity in log-log space, and a more straightforward analysis of their rotations over time could be carried out in semi-log space (see Fig 5) while clearly showing the inflection points on the evolutionary tracks of both early and mid-late M dwarfs that will be discussed later in this section.

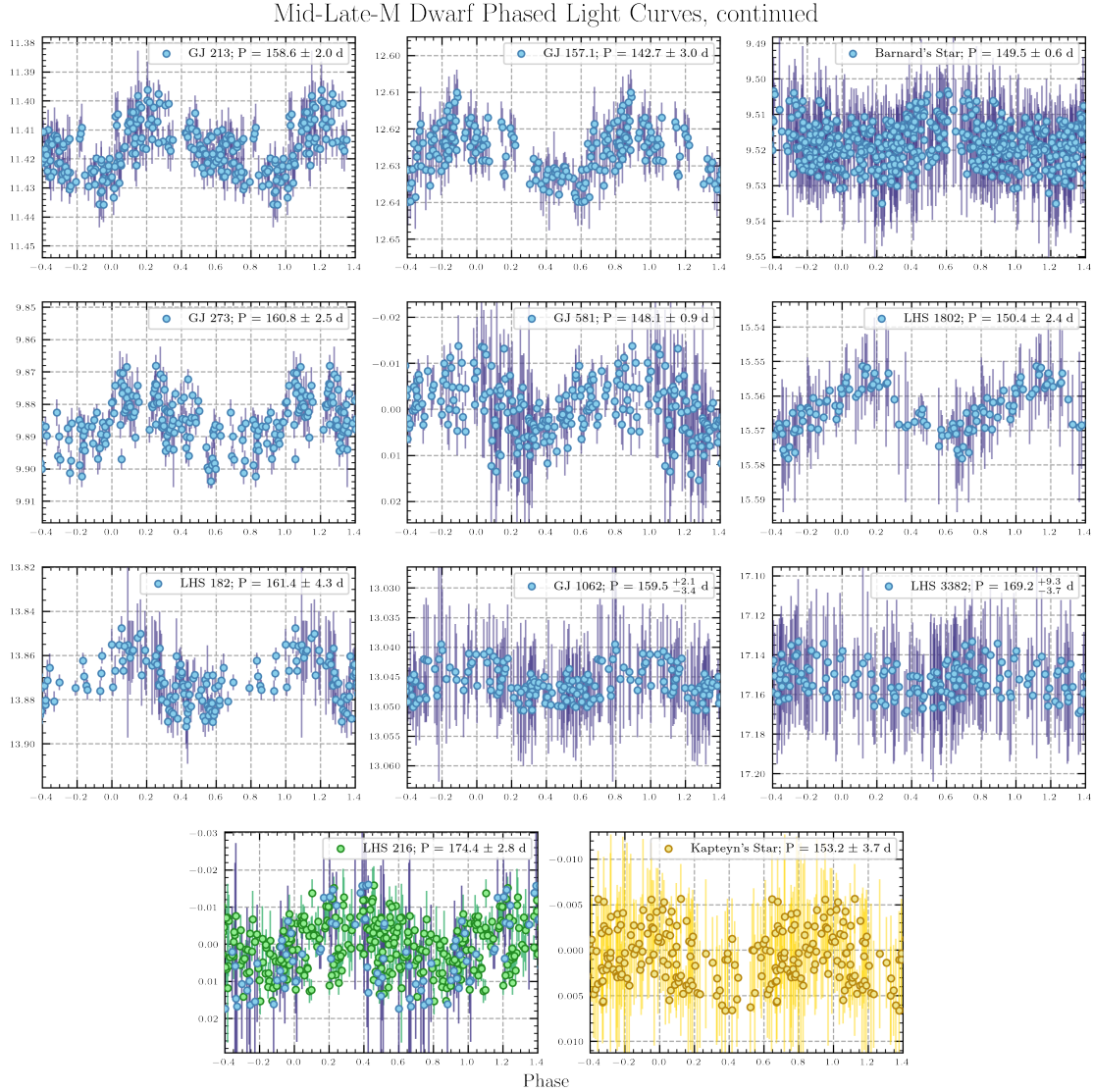


Figure 4. Additional phased rotation light curves of the mid-late M dwarf benchmarks, continued from and plotted in a similar fashion as Fig. 2.

As mentioned previously, constructing these relationships proved a rather complicated task, but not simply due to the difficulty in building a substantial set of benchmark targets and the observational burden of measuring their rotation periods. When it comes to spindown, it appears there is no way to broadly classify all M dwarfs; they represent too wide a range of parameters.

Table 1. The ‘Early’ M Dwarf (M0–2) Benchmarks

Name	Sp. Type	Age (Gyr)	P_{rot} (days)	Age determined via
Pleiades	M0-2V	0.125 [+0.05, -0.05]	2.05 [+2.96, -1.64] ¹	Cluster
NGC 2516	M2.5-6V	0.15 [+0.02, -0.02]	1.80 [+2.93, -1.50] ¹	Cluster
M34	M2.5-6V	0.22 [+0.02, -0.02]	6.85 [+6.51, -2.83] ¹	Cluster
NGC 3532	M0-2V	0.3 [+0.05, -0.05]	10.96 [+6.09, -9.26] ²	Cluster
M37	M0-2V	0.52 [+0.06, -0.06]	13.15 [+2.71, -9.03] ¹	Cluster
Praesepe / Hyades	M0-2V	0.73 [+0.12, -0.12]	16.06 [+2.48, -2.91] ³	Cluster
NGC 6811	M0-2V	1.0 [+0.2, -0.2]	12.6 [+1.74, -1.17] ⁴	Cluster
NGC 752	M0-2V	1.46 [+0.18, -0.18]	16.12 [+8.87, -13.83] ⁵	Cluster
LP 856-54	M1-1.5V	2.52 [+1.58, -0.62]	23.27 [+0.04, -0.04]	WD comp (LP 856-53)
Ruprecht 147	M0-2V	2.6 [+0.4, -0.4]	22.4 [+2.9, -2.9] ^{6,7}	Cluster
G 59-39	M0V	3.20 [+1.95, -0.93]	33.82 [+0.07, -0.07]	WD comp (EGGR 92)
GJ 2131 A	M1V	3.47 [+1.69, -0.33]	34.82 [+0.1, -0.1]	WD comp (GJ 2131 B)
LP 775-52	M0-1V	3.62 [+1.84, -0.34]	39.05 [+0.14, -0.14]	WD comp (LP 775-53)
G 111-72	M1.5-2V	3.64 [+1.35, -0.68]	38.96 [+0.13, -0.13]	WD comp (G 111-71)
HIP 43232 B	M1.5V	3.95 [+0.35, -0.35] ⁸	41.3 [+4.1, -4.1] ⁸	MS comp (HIP 43232 A)
LP 587-54	M1.5-2V	6.34 [+1.01, -0.94]	54.3 [+0.5, -0.5]	WD comp (LP 587-53)
GJ 366	M1.5V	9.5 [+1.5, -1.5]	87.1 [+1.4, -1.4]	Thick Disk/Halo Population
GJ 328	M0V	9.5 [+1.5, -1.5]	80.5 [+1.2, -1.2]	Thick Disk/Halo Population
GJ 821	M1V	9.5 [+1.5, -1.5]	86.2 [+0.6, -0.6]	Thick Disk/Halo Population
LP 552-48	M0V	9.88 [+1.77, -1.07]	92.9 [+1.3, -1.3]	WD comp (LP 552-49)
LHS 343	sdK7	11.5 [+1.0, -1.5]	89.2 [+1.7, -1.7]	Halo Population
LHS 173	esdK7 ⁹	11.5 [+1.0, -1.5]	85.3 [+3.4, -3.4]	Halo Population
LHS 174	sdM0 ⁹	11.5 [+1.0, -1.5]	90.4 [+1.5, -1.5]	Halo Population

NOTE— ¹Godoy-Rivera et al. (2021) ²Fritzewski et al. (2021) ³Núñez et al. (2022) ⁴Curtis et al. (2019) ⁵Agüeros et al. (2018) ^{6,7}Curtis et al. (2020); Gruner & Barnes (2020) ⁸Sawczynec, E. (2021), Thesis available at https://www.phys.hawaii.edu/wp-content/uploads/2021/06/ESawczynec_Thesis-1.pdf ⁹Kesseli et al. (2019)

Table 2. The ‘Mid’ M Dwarf (M2.5–6.5) Benchmarks

Name	Sp. Type	Age (Gyr)	P_{rot} (days)	Age determined via
Pleiades	M2.5–~6.5V ¹	0.125 [+0.05, -0.05]	0.59 [+0.65, -0.28] ²	Cluster
NGC 2516	M2.5-6V	0.15 [+0.02, -0.02]	0.68 [+0.77, -0.30] ²	Cluster
M34	M2.5-6V	0.22 [+0.02, -0.02]	3.03 [+3.58, -2.10] ²	Cluster
M37	M2.5-6V	0.52 [+0.06, -0.06]	7.66 [+5.61, -5.61] ²	Cluster
Praesepe / Hyades	M2.5–~6.5V ¹	0.73 [+0.12, -0.12]	23.8 [+3.3, -3.3] ³	Cluster
NGC 752	M2.5-6V	1.46 [+0.18, -0.18]	14.4 [+9.4, -4.7] ⁴	Cluster
NSV 11919	M2.5-3V	1.97 [+0.98, -0.35]	21.07 [+0.05, -0.05]	WD comp (NSV 11920)
Gaia DR3 7552 ^{5a}	M3-3.5V	1.98 [+1.01, -0.39]	20.6 [+1.1, -1.1]	WD comp (Gaia DR3 4784 ^{5b})
G 148-6	M3-3.5V	2.20 [+1.35, -0.57]	22.7 [+0.05, -0.05]	WD comp (G 148-7)
Ruprecht 147	M2.5-4V	2.6 [+0.4, -0.4]	25.3 [+6.9, -2.9]	Cluster
LP 783-2	M6.5V	3.12 [+1.73, -0.56]	25.45 [+0.06, -0.06]	WD comp (LP 783-3)
G 130-6	M3V	3.60 [+1.84, -1.63]	49.5 [+0.1, -0.1]	WD comp (G 130-5)
LP 498-25	M2.5V	3.80 [+0.70, -1.58]	49.0 [+0.2, -0.2]	WD comp (LP 498-26)
LHS 353	M4V	4.42 [+2.13, -1.52]	61.2 [+2.1, -2.1]	WD comp (GJ 515)
40 Eri C	M4.5V	4.89 [+4.81, -2.71]	81.0 [+0.7, -0.7]	WD comp (40 Eri B)
G 87-28	M4V	4.91 [+3.72, -2.65]	91.1 [+0.7, -0.7]	WD comp (G 87-29)
G 201-40	M3-3.5V	5.16 [+3.77, -2.86]	77.6 [+0.9, -0.9]	WD comp (G 201-39)
Proxima Cen	M5.5V	5.3 [+0.7, -0.7]	86.4 [+2.5, -2.5]	α Cen system
LSPM J1604+3909W	M4V	6.9 [+0.9, -0.9]	127.9 [+2.8, -2.8]	MS comp (HD 144579)
LHS 229	M4V	8.71 [+0.56, -0.46]	152.3[+1.7, -1.7]	WD comp (LHS 230)
GJ 299	M4.5V	9.5 [+1.5, -1.5]	156.9 [+1.2, -1.2]	Thick Disk/Halo Population
GJ 213	M4V	9.5 [+1.5, -1.5]	158.6 [+2.0, -2.0]	Thick Disk/Halo Population
GJ 157.1	M4V	9.5 [+1.5, -1.5]	142.7 [+3.0, -3.0]	Thick Disk/Halo Population
Barnard’s Star (GJ 699)	M4V	9.5 [+1.5, -1.5]	149.5 [+0.6, -0.6]	Thick Disk/Halo Population
GJ 273	M3.5V	9.5 [+1.5, -1.5]	160.8 [+2.5, -2.5]	Thick Disk/Halo Population
GJ 581	M3V	9.5 [+1.5, -1.5]	148.1 [+0.9, -0.9]	Thick Disk/Halo Population
LHS 1802	M5V	9.97 [+3.53, -5.12]	150.4 [+2.4, -2.4]	WD comp (LHS 1801)
LHS 182	usdM0	11.5 [+1.0, -1.5]	161.4 [+4.3, -4.3]	Halo Population
GJ 1062	sdM2.5	11.5 [+1.0, -1.5]	159.5 [+2.1, -3.4]	Halo Population
LHS 3382	esdM2.5	11.5 [+1.0, -1.5]	169.2 [+9.3, -3.7]	Halo Population
LHS 216	esdM3 ⁶	11.5 [+1.0, -1.5]	174.4 [+2.8, -2.8]	Halo Population

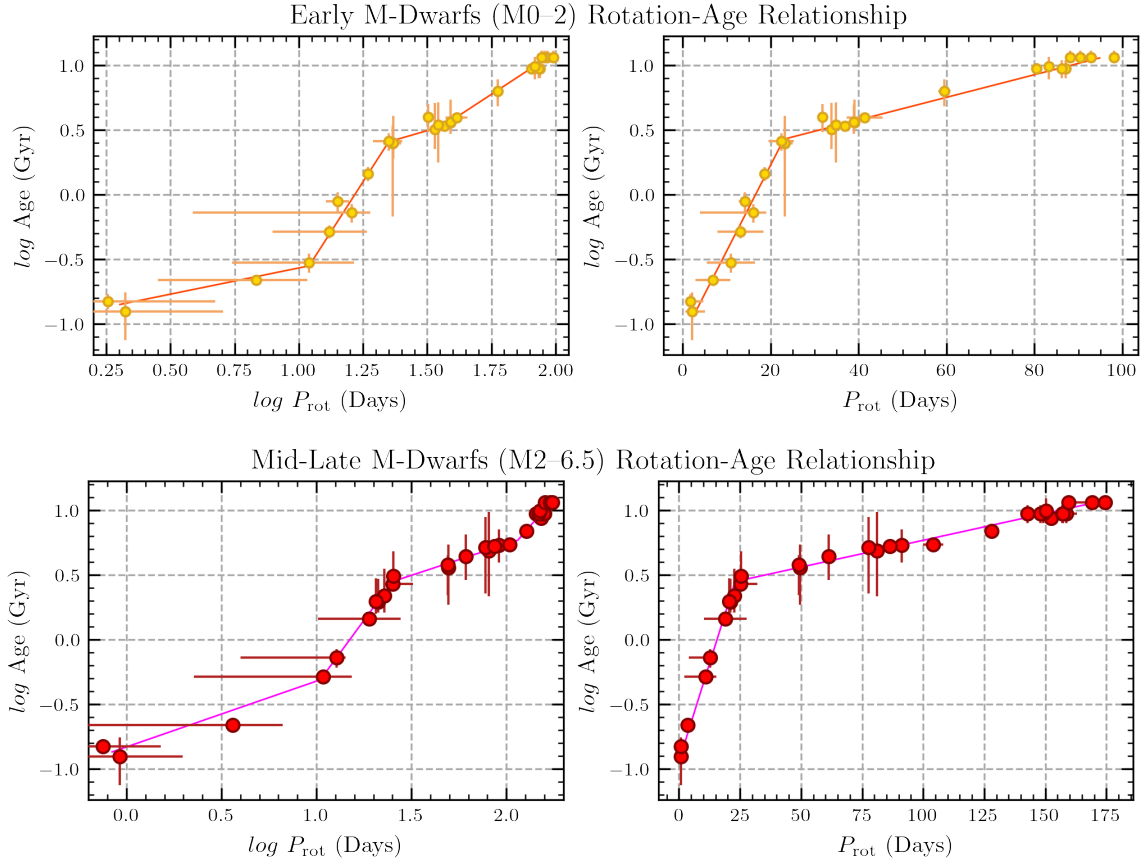


Figure 5. Plots showing log-log (left) vs semi-log (right) Age vs. Rotation relationships for the early (top) and mid-late (bottom) M dwarfs. As shown in the plots, the data of both groups are better linearized in semi-log form. It is perhaps possible that each ‘segment’ of the log-log plots represents a real evolutionary stage – e.g., the first segment is pre-main sequence evolution and the second represents the interiors of the M dwarfs synchronizing – and the semi-log plots merge these two distinct stages. However, given the current data and spread of rotation rates in the clusters, such a firm conclusion can’t be drawn here.

If you group together G dwarfs, the masses can vary by $\sim 10\%$. Grouping together all K dwarfs, the mass can vary by $\sim 30 - 40\%$. But studying M dwarfs, even focusing only on M0 – 6.5 dwarfs as we have done here, the mass can vary by $> 500\%$. Important changes occur within the stars’ interior

Table 3. Parameters Used to Derive Ages for the White Dwarf Companions

WD Name	WD Type	Model	$\log g$	T_{eff}	Source(s)
LP 856-53	DA5	H Thick	8.12 [+0.08, -0.08]	9903 [+105, -105]	6, 17, 18, 19
GJ 2131 B	DA3.9	H Thick	7.98 [+0.03, -0.03]	12615 [+420, -420]	6, 9, 17
G 111-71	DA6.5	H Thick	8.01 [+0.08, -0.08]	7560 [+23, -24]	4, 6, 9, 18
LP 775-53	DA	H Thick	8.085 [+0.125, -0.125]	6587 [+100, -100]	6, 18
EGGR 92	DA4	H Thick	8.01 [+0.04, -0.04]	10590 [+65, -65]	3, 6, 18
LP 587-53	DA8.6	H Thick	7.96 [+0.03, -0.02]	5782 [+73, -82]	3, 4, 6
LP 552-49	DC	H Thin	8.00 [+0.25, -0.25]	4460 [+106, -106]	4, 13
NSV 11920	DBZ5	H Thin	8.105 [+0.02, -0.02]	11070 [+96, -96]	2, 7, 11, 16, 28, 29
Gaia DR3 4784	non-DA	H Thin	8.15 [-0.05, -0.05]	9960 [+112, -112]	28, 29
G 148-7	DA3.1	H Thick	8.01 [-0.02, -0.02]	15840 [+329, -329]	3, 6, 9, 13, 18, 26, 27
LP 783-3	DZ6.5	H Thin	8.10 [+0.03, -0.03]	7924 [+97, -97]	6, 11, 16, 21
G 130-5	DA4	H Thick	7.99 [+0.04, -0.04]	12838 [+180, -180]	3, 6, 9, 13, 18
LP 498-26	DB3	H Thin	8.02 [+0.05, -0.05]	15405 [+232, -232]	5, 6, 7
GJ 515	DA4	H Thick	7.94 [+0.04, -0.04]	14405 [+200, -200]	9, 17, 19, 21, 28
LP 672-1	DA3.1	H Thick	7.94 [+0.03, -0.03]	15742 [+423, -423]	6, 17, 18, 19, 21
LHS 27	DC7.1	H Thin	8.14 [+0.03, -0.03]	7060 [+205, -205]	1, 13, 16, 25
40 Eri B	DA2.9	H Thin	7.94 [+0.04, -0.04]	16979 [+424, -424]	8, 9, 20
G 201-39	DA5.6	H Thick	7.97 [+0.06, -0.05]	9007 [+69, -70]	3, 6, 10, 17, 18
G 87-29	DQ8	H Thin	8.00 [+0.12, -0.12]	6674 [+360, -360]	4, 6, 13, 24, 25
LHS 230	DA+DA	H Thick	8.10 [+0.03, -0.27]	4926 [+255, -255]	12
LHS 1801	DA	H Thick	7.92 [+0.07, -0.06]	5145 [+88, -89]	4, 6, 13

NOTE— ¹McCleery et al. (2020) ²Klein et al. (2020) ³Kilic et al. (2020) ⁴Blouin et al. (2019) ⁵Kong et al. (2019) ⁶Gentile Fusillo et al. (2019) ⁷Rolland et al. (2018) ⁸Bond et al. (2017) ⁹Bédard et al. (2017) ¹⁰Anguiano et al. (2017) ¹¹Subasavage et al. (2017) ¹²Holberg et al. (2016) ¹³Limoges et al. (2015) ¹⁴Genest-Beaulieu & Bergeron (2014) ¹⁵Kawka & Vennes (2012) ¹⁶Giammichele et al. (2012) ¹⁷Gianninas et al. (2011) ¹⁸Garcés et al. (2011) ¹⁹Koester et al. (2009) ²⁰Holberg et al. (2008b) ²¹Holberg et al. (2008a) ²²Holberg & Bergeron (2006) ²³Castanheira et al. (2006) ²⁴Dufour et al. (2005) ²⁵Bergeron et al. (2001) ²⁶Bergeron et al. (1995) ²⁷Bergeron et al. (1992) ²⁸Gentile Fusillo et al. (2021) ²⁹Jiménez-Esteban et al. (2023)

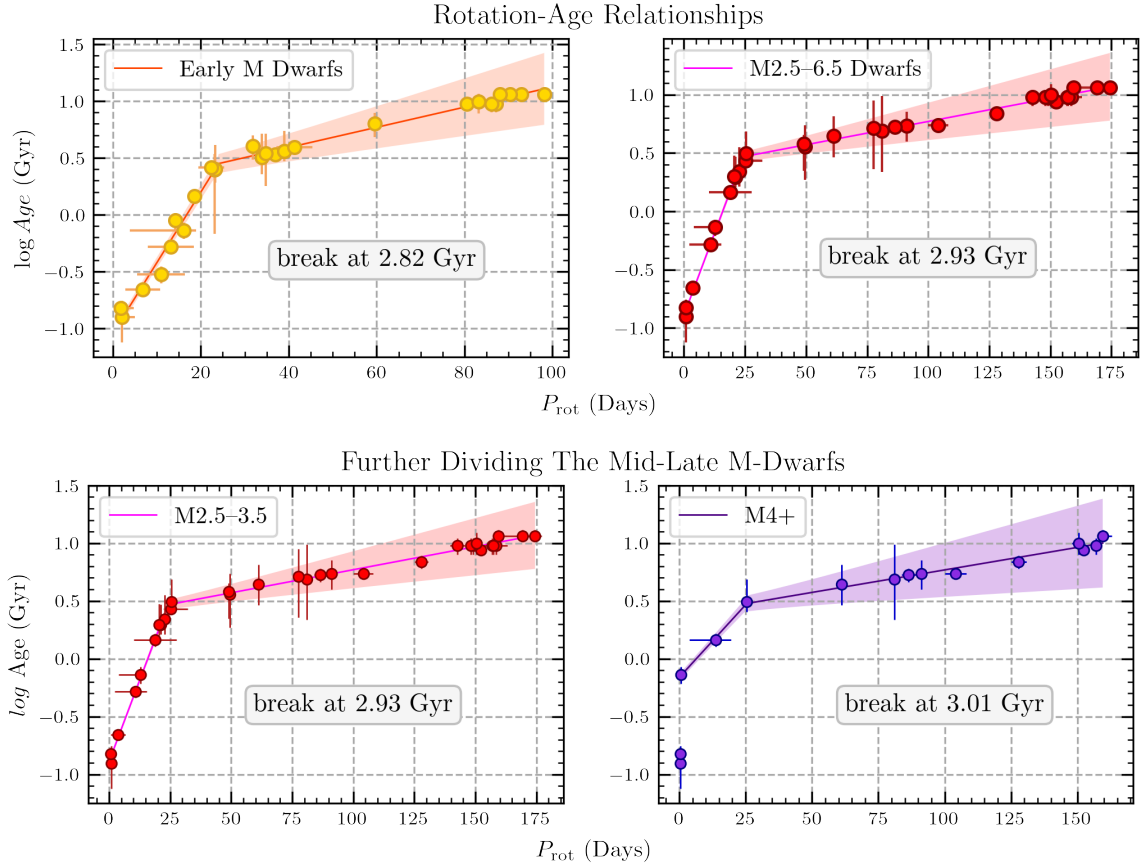


Figure 6. Age-Rotation relationships are plotted for the different M dwarf subsets, in semi-log space. In the top left, only the early (M0 – 2) subset is plotted. In the top right, the mid-late subset is plotted. This subset contains M2.5 – 6.5 dwarfs except on the young track where only M2.5 – 3.5 dwarfs are plotted. In the bottom left, the mid-late plot is repeated, with M2.5 – 3.5 dwarfs on the younger track and M2.5 – 6.5 dwarfs on the older track. Finally, in the bottom right, the relationships for M4 and later spectral types is plotted. Clear inflection points can be seen in the plots of all stellar subsets. This is believed to occur when the interiors of the stars re-synchronize, and the next phase of their rotational evolution can begin. Also note the drastically different rotation-scales for each subset, with the oldest early M dwarfs slowing to 100 days, yet the mid-late M dwarfs slow much further, to 175 day rotation periods.

structures and evolutionary timelines, which can be observed (and need to be accounted for) in the rotation relationships.

One dramatic difference was suspected early in the study, but required lengthy follow-up. Preliminary project results showed the rotations of (especially older) early vs. mid-late M dwarfs followed divergent evolutionary paths (Engle & Guinan 2018) as they aged. This splitting of M dwarf subsets

into distinct rotation-based groups has been observed in other studies, as well (see [Popinchalk et al. 2021](#)). Also particularly relevant to this study; models have shown (Louis Amard, private communication) that the oldest stars (subdwarf members of the Halo population) display an interesting and related phenomenon where their interiors are structured as that of a main sequence star with slightly later spectral type (see [Tables 1 and 2](#)). An example is Kapteyn’s Star, which would initially be considered a member of our early subset since it is classified as sdM1.5, yet models indicate it has a fully convective interior similar to a \sim M2.5 or later main sequence star. A potential explanation for subdwarfs having deeper convective zones than their spectral types would indicate is that their smaller radii lead to larger interior temperature gradients, but confirming the true cause requires further study.

By an age of 10 Gyr, the average mid-late M dwarf will have a rotation period almost twice as long as the average early M dwarf (\sim 155 vs \sim 85 days – see [Figs 5 & 6](#)). These different paths resulted in our first subdivision of the M dwarfs, into what we call the ‘early’ (M0 – 2) and ‘mid-late’ (M2.5 – 6.5) groups. This is near to, but earlier than, the usual spectral type of M3 – 3.5 which is routinely quoted as the transition point to a fully convective interior. [Mullan & Houdebine \(2020\)](#) recently showed, however, that changes due to magnetic effects (which would be rotation-related) likely occur within the M2.1 – 2.3 range, which is encouraging in light of our rotation period results. The decision to not include stars with spectral types later than \sim M6.5 V is intentional. First, we presently do not have a sufficient sample of older stars at these later spectral types with both well-determined ages and rotation periods. Second, from the small sample of such stars that is available, it appears they either experience no appreciable spindown effect, or one that is altogether different from any of the other M dwarf subsets presented here. A well-known example is the M8 V star Trappist-1, that has an age of 7.6 ± 2.2 Gyr and a rotation period of 3.39 days (e.g., [Burgasser & Mamajek 2017](#)).

There is an additional complication at young ages, due to the length of time required for each star to reach the main sequence. As with other issues, this one is also particularly difficult for M dwarfs, whose pre-main sequence lifetimes can range from \sim 140 Myr to \sim 1.5 Gyr (M0 – 6.5 dwarfs [Choi et al. 2016](#)). Due to this, on top of the spread of initial rotation rates normally displayed by all

cool dwarf stars, younger M dwarfs show a larger range of rotation periods, as detailed in several excellent studies (see [Douglas et al. 2019](#); [Gruner & Barnes 2020](#); [Curtis et al. 2020](#); [Godoy-Rivera et al. 2021](#) for recent examples). After an age of ~ 3 Gyr, all mid-late M dwarfs have converged onto a single evolutionary track, and any differences between their rotation-determined ages are negligible compared to the uncertainties of the relationships. At young ages, though, this group appears to require further subdivision, most likely as a result of lengthening pre-main sequence lifetimes. Due to the distances of some of these young clusters, this aspect of the study is in need of further study, but M dwarfs later than $\sim M4$ sensibly appear to follow a different evolutionary path while young (the bottom plots of Fig 6 show this further subdivision).

Previous studies (see [Curtis et al. 2020](#)) have proposed the rotation periods of cool dwarfs do not follow one continuous evolutionary track, characterized by a single powerlaw relationship ($P_{\text{rot}} \propto \text{Age}^n$), with a ‘braking index’ determined by the exponent (n). This was originally proposed by [Skumanich \(1972\)](#), with an initially determined value of $n = 0.5$ for that study’s target sample, and recent studies have revised this value. [Douglas et al. \(2019\)](#) and [Dungee et al. \(2022\)](#), for example, each derived an index of $n \approx 0.62$, although [Douglas et al.](#) studied only F and G dwarfs – more massive than the stars studied here – but [Dungee et al.](#) included stars up to $\sim M3$.

For these data, and the activity-age relationships in the following subsections, a two-segment linear equation was defined using the `numpy.piecewise` function and fit to each data set using `scipy.optimize.least_squares`. The final, fitted age-rotation relationships are shown in Fig 6 with the best-fitting parameters:

M0–2 dwarfs:

$$\log Age (Gyr) = 0.0621[0.0025] \times P_{\text{rot}} (days) - 1.0437[0.0394]$$

$$\text{for } P_{\text{rot}} < 24.0379[0.8042]$$

$$\log Age (Gyr) = 0.0621[0.0025] \times P_{\text{rot}} (days) - 1.0437[0.0394]$$

$$- 0.0533[0.0026] \times (P_{\text{rot}} - 24.0379[0.8042])$$

$$\text{for } P_{\text{rot}} \geq 24.0379[0.8042]$$

(1)

M2.5–3.5 dwarfs [M2.5 – M6.5, if $P_{\text{rot}} \gtrsim 24.18$]:

$$\log Age (Gyr) = 0.0561[0.0012] \times P_{\text{rot}} (days) - 0.8900[0.0188]$$

$$\text{for } P_{\text{rot}} < 24.1823[0.4384]$$

$$\log Age (Gyr) = 0.0561[0.0012] \times P_{\text{rot}} (days) - 0.8900[0.0188]$$

$$- 0.0521[0.0013] \times (P_{\text{rot}} - 24.1823[0.4384])$$

$$\text{for } P_{\text{rot}} \geq 24.1823[0.4384]$$

(2)

M4 – 6.5 dwarfs:

$$\log Age (Gyr) = 0.0251[0.0022] \times P_{\text{rot}} (days) - 0.1615[0.0309]$$

$$\text{for } P_{\text{rot}} < 25.4500[2.4552]$$

$$\log Age (Gyr) = 0.0251[0.0022] \times P_{\text{rot}} (days) - 0.1615[0.0309]$$

$$- 0.0212[0.0022] \times (P_{\text{rot}} - 25.4500[2.4552])$$

$$\text{for } P_{\text{rot}} \geq 25.4500[2.4552]$$

(3)

Together, these relationships cover M0–6.5 dwarfs. Within 10 pc of the Sun, this represents $\sim 72\%$ of all stars with known spectral types (and $\sim 48\%$ of the wider range of objects, including stellar remnants and brown dwarfs [Reylé et al. \(2021\)](#)). As mentioned early in the paper, an increasing number of M dwarfs are being discovered as exoplanet hosts. Determining the ages of these stars, and thus the ages of their exoplanets, is important when selecting the ideal targets to further study for evidence of habitability or even life. Single-celled organisms originated when the Earth (the only example we currently have for such events) was $\sim 0.7 - 0.9$ Gyr old. The Great Oxygenation of the atmosphere occurred when Earth was ~ 2.2 Gyr old, the Cambrian Explosion and rapid diversification of complex lifeforms when Earth was $\sim 4 - 4.1$ Gyr old, and technological civilization didn't occur until the Earth was >4.5 Gyr old. Thus, exoplanet age is an important discriminator in the search for life. To demonstrate a benefit of our relationships, we provide the gyrochronological ages for all \sim M0–6.5 dwarf exoplanet hosts with a listed rotation period in the *NASA Exoplanet Archive*² in Table 4. The follow-up paper ([Engle 2023](#)) will focus on the X-ray and UV activity of M dwarfs over time, and what insights these relationships offer for the stars, their magnetic dynamos, and their suitability to host potentially habitable planets.

We do wish to advise restraint, though, when using the first or ‘young’ tracks of these relationships. These ages were included to, as best we could, characterize the fullest evolutionary paths of average early to mid-late M dwarfs. However, as noted earlier in this section, M dwarfs display a *wide* range of rotation rates at young ages that are not represented by the relationship uncertainties (note the data point vs. relationship uncertainties along the ‘young’ tracks in Fig 6). Including estimates from activity-age relationships extends the reliable range of age determinations, and this is discussed in the companion paper.

[Barnes \(2003\)](#) theorized that the rotational evolution of main sequence stars showed two possible sequences, dependent on both time and mass (therefore spectral type). The two sequences were termed the Interface (I) and Convective (C) sequences, named after the magnetic dynamos and

² <https://exoplanetarchive.ipac.caltech.edu/>

interior structures of the stellar groups. The more massive, hotter stars spend only a short time on the C sequence before switching to the I sequence. On the I sequence, there is an interface between the radiative and convective regions of the stellar interior, but the magnetic field couples the regions together and much of the stellar interior rotates as a rigid body. Lower mass stars spend longer amounts of time on the C sequence before switching over, and fully convective stars likely never leave the C sequence. [Spada & Lanzafame \(2020\)](#) put forth an analytical model theorizing that stars do not initially evolve as rigid bodies. Rather, as the stellar surface loses angular momentum, a profile of differential rotation builds within the star. Angular momentum is transported from the interior to the surface and eventually the interior of the star ‘re-couples’. This accounts for the two-track evolutionary path where the second evolutionary track begins after the interior of the star has re-coupled. [Spada & Lanzafame](#) only calculated their model down to early M dwarf masses. At this mass range, however, the models predict that a ~ 4 Gyr old early M dwarf will have a $\sim 31 - 32$ day rotation period, where our data indicates a $\sim 40 - 45$ day period.

To determine the braking indices of our M dwarf subsets, and to serve as an additional comparison to literature results, rotation vs. age data were fitted in linear space with a two-segment powerlaw equation. A best fitting braking index (for the second evolutionary track) was determined to be 0.61 for the early M dwarfs and 0.62 for the mid-late M dwarfs; nearly identical to each other, well within the parameter uncertainties, and in excellent agreement with the results of [Douglas et al. \(2019\)](#) and [Dungee et al. \(2022\)](#). However, it is again worth noting that [Douglas et al. 2019](#) based their braking index determination on solar-like F and G dwarfs, and on a comparison of the Praesepe cluster and the Sun. Just over fifty years after [Skumanich \(1972\)](#) first discovered the spindown effect operating in solar-type G dwarfs, it is an interesting implication that all cool dwarfs, from late F to $\sim M6.5$, may perhaps spindown according to the same braking index but simply with different re-coupling timescales. Further investigation into the angular momentum loss of M dwarfs, using methods such as those of [See et al. \(2019\)](#) and [Barnes & Kim \(2010\)](#) and comparisons between measures and estimated magnetic field strengths and mass loss rates, are underway for inclusion in a follow-up paper.

These data and relationships will be of great use to the field and offer valuable insights into the most populous stellar members of our galaxy, M dwarfs. They allow for reliable ages and evolutionary histories to be determined, but may also offer further insight into the differing dynamo mechanisms at work within the M dwarf subsets and how each mechanism influences, or responds to, the star's evolution over time.

5. ACKNOWLEDGEMENTS

We would like to acknowledge the tireless work of the *RCT Consortium* members, including former members David Laney and Louis-Gregory Strolger, for the operation and maintenance of the telescope and equipment, without which this study would not have been possible. We also wish to acknowledge the builders and operators of the *Skynet* telescope network and the *Zwicky Transient Facility*. Partial support for this project was provided by CXO grant GO0-21020X.

SGE thanks Louis Amard for invaluable discussions and access to his M dwarf interior models. SGE also thanks Andrej Prša for very helpful discussions regarding the regression fitting.

Facilities: KPNO:RCT, CTIO:PROMPT

Software: `astropy` (Astropy Collaboration et al. 2013, 2018, 2022), `Matplotlib` (Hunter 2007), `Pandas` (pandas development team 2020), `NumPy` (Harris et al. 2020), `SciPy` (Virtanen et al. 2020), `AstroImageJ` (Collins et al. 2017)

REFERENCES

- Agüeros, M. A., Bowsher, E. C., Bochanski, J. J., et al. 2018, *ApJ*, 862, 33, doi: [10.3847/1538-4357/aac6ed](https://doi.org/10.3847/1538-4357/aac6ed)
- Anguiano, B., Rebassa-Mansergas, A., García-Berro, E., et al. 2017, *MNRAS*, 469, 2102, doi: [10.1093/mnras/stx796](https://doi.org/10.1093/mnras/stx796)
- Astropy Collaboration, Robitaille, T. P., Tollerud, E. J., et al. 2013, *A&A*, 558, A33, doi: [10.1051/0004-6361/201322068](https://doi.org/10.1051/0004-6361/201322068)
- Astropy Collaboration, Price-Whelan, A. M., Sipócz, B. M., et al. 2018, *AJ*, 156, 123, doi: [10.3847/1538-3881/aabc4f](https://doi.org/10.3847/1538-3881/aabc4f)
- Astropy Collaboration, Price-Whelan, A. M., Lim, P. L., et al. 2022, *ApJ*, 935, 167, doi: [10.3847/1538-4357/ac7c74](https://doi.org/10.3847/1538-4357/ac7c74)
- Barnes, S. A. 2003, *ApJ*, 586, 464, doi: [10.1086/367639](https://doi.org/10.1086/367639)
- . 2007, *ApJ*, 669, 1167, doi: [10.1086/519295](https://doi.org/10.1086/519295)
- Barnes, S. A., & Kim, Y.-C. 2010, *ApJ*, 721, 675, doi: [10.1088/0004-637X/721/1/675](https://doi.org/10.1088/0004-637X/721/1/675)
- Bédard, A., Bergeron, P., Brassard, P., & Fontaine, G. 2020, *ApJ*, 901, 93, doi: [10.3847/1538-4357/abafbe](https://doi.org/10.3847/1538-4357/abafbe)
- Bédard, A., Bergeron, P., & Fontaine, G. 2017, *ApJ*, 848, 11, doi: [10.3847/1538-4357/aa8bb6](https://doi.org/10.3847/1538-4357/aa8bb6)
- Bensby, T., Feltzing, S., & Oey, M. S. 2014, *A&A*, 562, A71, doi: [10.1051/0004-6361/201322631](https://doi.org/10.1051/0004-6361/201322631)
- Bergeron, P., Leggett, S. K., & Ruiz, M. T. 2001, *ApJS*, 133, 413, doi: [10.1086/320356](https://doi.org/10.1086/320356)
- Bergeron, P., Liebert, J., & Fulbright, M. S. 1995, *ApJ*, 444, 810, doi: [10.1086/175654](https://doi.org/10.1086/175654)
- Bergeron, P., Saffer, R. A., & Liebert, J. 1992, *ApJ*, 394, 228, doi: [10.1086/171575](https://doi.org/10.1086/171575)
- Blouin, S., Dufour, P., Thibeault, C., & Allard, N. F. 2019, *ApJ*, 878, 63, doi: [10.3847/1538-4357/ab1f82](https://doi.org/10.3847/1538-4357/ab1f82)
- Bond, H. E., Bergeron, P., & Bédard, A. 2017, *ApJ*, 848, 16, doi: [10.3847/1538-4357/aa8a63](https://doi.org/10.3847/1538-4357/aa8a63)
- Burgasser, A. J., & Mamajek, E. E. 2017, *ApJ*, 845, 110, doi: [10.3847/1538-4357/aa7fea](https://doi.org/10.3847/1538-4357/aa7fea)
- Castanheira, B. G., Kepler, S. O., Handler, G., & Koester, D. 2006, *A&A*, 450, 331, doi: [10.1051/0004-6361:20054221](https://doi.org/10.1051/0004-6361:20054221)
- Choi, J., Dotter, A., Conroy, C., et al. 2016, *ApJ*, 823, 102, doi: [10.3847/0004-637X/823/2/102](https://doi.org/10.3847/0004-637X/823/2/102)
- Collins, K. A., Kielkopf, J. F., Stassun, K. G., & Hessman, F. V. 2017, *AJ*, 153, 77, doi: [10.3847/1538-3881/153/2/77](https://doi.org/10.3847/1538-3881/153/2/77)
- Cummings, J. D., Kalirai, J. S., Tremblay, P. E., Ramirez-Ruiz, E., & Choi, J. 2018, *ApJ*, 866, 21, doi: [10.3847/1538-4357/aadfd6](https://doi.org/10.3847/1538-4357/aadfd6)
- Curtis, J. L., Agüeros, M. A., Douglas, S. T., & Meibom, S. 2019, *ApJ*, 879, 49, doi: [10.3847/1538-4357/ab2393](https://doi.org/10.3847/1538-4357/ab2393)
- Curtis, J. L., Agüeros, M. A., Matt, S. P., et al. 2020, *ApJ*, 904, 140, doi: [10.3847/1538-4357/abbbf58](https://doi.org/10.3847/1538-4357/abbbf58)
- Douglas, S. T., Curtis, J. L., Agüeros, M. A., et al. 2019, *ApJ*, 879, 100, doi: [10.3847/1538-4357/ab2468](https://doi.org/10.3847/1538-4357/ab2468)
- Dressing, C. D., & Charbonneau, D. 2013, *ApJ*, 767, 95, doi: [10.1088/0004-637X/767/1/95](https://doi.org/10.1088/0004-637X/767/1/95)

- Dufour, P., Bergeron, P., & Fontaine, G. 2005, *ApJ*, 627, 404, doi: [10.1086/430373](https://doi.org/10.1086/430373)
- Dungee, R., van Saders, J., Gaidos, E., et al. 2022, *ApJ*, 938, 118, doi: [10.3847/1538-4357/ac90be](https://doi.org/10.3847/1538-4357/ac90be)
- Engle, S. 2015, PhD thesis, James Cook University, Australia
- Engle, S. G., & Guinan, E. F. 2011, in *Astronomical Society of the Pacific Conference Series*, Vol. 451, 9th Pacific Rim Conference on Stellar Astrophysics, ed. S. Qain, K. Leung, L. Zhu, & S. Kwok, 285, doi: [10.48550/arXiv.1111.2872](https://doi.org/10.48550/arXiv.1111.2872)
- Engle, S. G., & Guinan, E. F. 2018, *Research Notes of the American Astronomical Society*, 2, 34, doi: [10.3847/2515-5172/aab1f8](https://doi.org/10.3847/2515-5172/aab1f8)
- France, K., Duvvuri, G., Egan, H., et al. 2020, *AJ*, 160, 237, doi: [10.3847/1538-3881/abb465](https://doi.org/10.3847/1538-3881/abb465)
- Fritzewski, D. J., Barnes, S. A., James, D. J., & Strassmeier, K. G. 2021, *A&A*, 652, A60, doi: [10.1051/0004-6361/202140894](https://doi.org/10.1051/0004-6361/202140894)
- Garcés, A., Catalán, S., & Ribas, I. 2011, *A&A*, 531, A7, doi: [10.1051/0004-6361/201116775](https://doi.org/10.1051/0004-6361/201116775)
- Genest-Beaulieu, C., & Bergeron, P. 2014, *ApJ*, 796, 128, doi: [10.1088/0004-637X/796/2/128](https://doi.org/10.1088/0004-637X/796/2/128)
- Gentile Fusillo, N. P., Tremblay, P.-E., Gänsicke, B. T., et al. 2019, *MNRAS*, 482, 4570, doi: [10.1093/mnras/sty3016](https://doi.org/10.1093/mnras/sty3016)
- Gentile Fusillo, N. P., Tremblay, P. E., Cukanovaite, E., et al. 2021, *MNRAS*, 508, 3877, doi: [10.1093/mnras/stab2672](https://doi.org/10.1093/mnras/stab2672)
- Giammichele, N., Bergeron, P., & Dufour, P. 2012, *ApJS*, 199, 29, doi: [10.1088/0067-0049/199/2/29](https://doi.org/10.1088/0067-0049/199/2/29)
- Gianninas, A., Bergeron, P., & Ruiz, M. T. 2011, *ApJ*, 743, 138, doi: [10.1088/0004-637X/743/2/138](https://doi.org/10.1088/0004-637X/743/2/138)
- Gizis, J. E. 1997, *AJ*, 113, 806, doi: [10.1086/118302](https://doi.org/10.1086/118302)
- Godoy-Rivera, D., Pinsonneault, M. H., & Rebull, L. M. 2021, *ApJS*, 257, 46, doi: [10.3847/1538-4365/ac2058](https://doi.org/10.3847/1538-4365/ac2058)
- Gruner, D., & Barnes, S. A. 2020, *A&A*, 644, A16, doi: [10.1051/0004-6361/202038984](https://doi.org/10.1051/0004-6361/202038984)
- Harris, C. R., Millman, K. J., van der Walt, S. J., et al. 2020, *Nature*, 585, 357, doi: [10.1038/s41586-020-2649-2](https://doi.org/10.1038/s41586-020-2649-2)
- Holberg, J. B., & Bergeron, P. 2006, *AJ*, 132, 1221, doi: [10.1086/505938](https://doi.org/10.1086/505938)
- Holberg, J. B., Bergeron, P., & Gianninas, A. 2008a, *AJ*, 135, 1239, doi: [10.1088/0004-6256/135/4/1239](https://doi.org/10.1088/0004-6256/135/4/1239)
- Holberg, J. B., Oswalt, T. D., Sion, E. M., & McCook, G. P. 2016, *MNRAS*, 462, 2295, doi: [10.1093/mnras/stw1357](https://doi.org/10.1093/mnras/stw1357)
- Holberg, J. B., Sion, E. M., Oswalt, T., et al. 2008b, *AJ*, 135, 1225, doi: [10.1088/0004-6256/135/4/1225](https://doi.org/10.1088/0004-6256/135/4/1225)
- Hsu, D. C., Ford, E. B., & Terrien, R. 2020, *MNRAS*, 498, 2249, doi: [10.1093/mnras/staa2391](https://doi.org/10.1093/mnras/staa2391)
- Hunter, J. D. 2007, *Computing in Science ‘&’ Engineering*, 9, 90, doi: [10.1109/MCSE.2007.55](https://doi.org/10.1109/MCSE.2007.55)
- IRSA. 2022, *Time Series Tool*, IPAC, doi: [10.26131/IRSA538](https://doi.org/10.26131/IRSA538)

- Jiménez-Esteban, F. M., Torres, S.,
Rebassa-Mansergas, A., et al. 2023, MNRAS,
518, 5106, doi: [10.1093/mnras/stac3382](https://doi.org/10.1093/mnras/stac3382)
- Kawaler, S. D. 1988, ApJ, 333, 236,
doi: [10.1086/166740](https://doi.org/10.1086/166740)
- Kawka, A., & Vennes, S. 2012, MNRAS, 425,
1394, doi: [10.1111/j.1365-2966.2012.21574.x](https://doi.org/10.1111/j.1365-2966.2012.21574.x)
- Kesseli, A. Y., Kirkpatrick, J. D., Fajardo-Acosta,
S. B., et al. 2019, AJ, 157, 63,
doi: [10.3847/1538-3881/aae982](https://doi.org/10.3847/1538-3881/aae982)
- Kilic, M., Bergeron, P., Kosakowski, A., et al.
2020, ApJ, 898, 84,
doi: [10.3847/1538-4357/ab9b8d](https://doi.org/10.3847/1538-4357/ab9b8d)
- Kimán, R., Xu, S., Faherty, J. K., et al. 2022, AJ,
164, 62, doi: [10.3847/1538-3881/ac7788](https://doi.org/10.3847/1538-3881/ac7788)
- Klein, B., Blouin, S., Romani, D., et al. 2020, ApJ,
900, 2, doi: [10.3847/1538-4357/ab9b24](https://doi.org/10.3847/1538-4357/ab9b24)
- Koester, D., Voss, B., Napiwotzki, R., et al. 2009,
A&A, 505, 441,
doi: [10.1051/0004-6361/200912531](https://doi.org/10.1051/0004-6361/200912531)
- Kong, X., Luo, A. L., & Li, X.-R. 2019, Research
in Astronomy and Astrophysics, 19, 088,
doi: [10.1088/1674-4527/19/6/88](https://doi.org/10.1088/1674-4527/19/6/88)
- Kopparapu, R. K. 2013, ApJL, 767, L8,
doi: [10.1088/2041-8205/767/1/L8](https://doi.org/10.1088/2041-8205/767/1/L8)
- Kushniruk, I., Bensby, T., Feltzing, S., et al. 2020,
A&A, 638, A154,
doi: [10.1051/0004-6361/202037923](https://doi.org/10.1051/0004-6361/202037923)
- Leggett, S. K., Ruiz, M. T., & Bergeron, P. 1998,
ApJ, 497, 294, doi: [10.1086/305463](https://doi.org/10.1086/305463)
- Limoges, M. M., Bergeron, P., & Lépine, S. 2015,
ApJS, 219, 19, doi: [10.1088/0067-0049/219/2/19](https://doi.org/10.1088/0067-0049/219/2/19)
- Lu, Y. L., Angus, R., Curtis, J. L., David, T. J., &
Kimán, R. 2021, AJ, 161, 189,
doi: [10.3847/1538-3881/abe4d6](https://doi.org/10.3847/1538-3881/abe4d6)
- Mamajek, E. E., & Hillenbrand, L. A. 2008, ApJ,
687, 1264, doi: [10.1086/591785](https://doi.org/10.1086/591785)
- McCleery, J., Tremblay, P.-E., Gentile Fusillo,
N. P., et al. 2020, MNRAS, 499, 1890,
doi: [10.1093/mnras/staa2030](https://doi.org/10.1093/mnras/staa2030)
- Mullan, D. J., & Houdebine, E. R. 2020, ApJ, 891,
128, doi: [10.3847/1538-4357/ab6ffa](https://doi.org/10.3847/1538-4357/ab6ffa)
- Núñez, A., Agüeros, M. A., Covey, K. R., et al.
2022, ApJ, 931, 45,
doi: [10.3847/1538-4357/ac6517](https://doi.org/10.3847/1538-4357/ac6517)
- pandas development team, T. 2020,
pandas-dev/pandas: Pandas, latest, Zenodo,
doi: [10.5281/zenodo.3509134](https://doi.org/10.5281/zenodo.3509134)
- Pass, E. K., Charbonneau, D., Irwin, J. M., &
Winters, J. G. 2022, ApJ, 936, 109,
doi: [10.3847/1538-4357/ac7da8](https://doi.org/10.3847/1538-4357/ac7da8)
- Paunzen, E., & Vanmunster, T. 2016,
Astronomische Nachrichten, 337, 239,
doi: [10.1002/asna.201512254](https://doi.org/10.1002/asna.201512254)
- Popinchalk, M., Faherty, J. K., Kimán, R., et al.
2021, ApJ, 916, 77,
doi: [10.3847/1538-4357/ac0444](https://doi.org/10.3847/1538-4357/ac0444)
- Reylé, C., Jardine, K., Fouqué, P., et al. 2021,
A&A, 650, A201,
doi: [10.1051/0004-6361/202140985](https://doi.org/10.1051/0004-6361/202140985)
- Robertson, P., Stefansson, G., Mahadevan, S.,
et al. 2020, ApJ, 897, 125,
doi: [10.3847/1538-4357/ab989f](https://doi.org/10.3847/1538-4357/ab989f)

- Rojas-Ayala, B. 2023, arXiv e-prints,
arXiv:2301.03442,
doi: [10.48550/arXiv.2301.03442](https://doi.org/10.48550/arXiv.2301.03442)
- Rolland, B., Bergeron, P., & Fontaine, G. 2018,
ApJ, 857, 56, doi: [10.3847/1538-4357/aab713](https://doi.org/10.3847/1538-4357/aab713)
- See, V., Matt, S. P., Finley, A. J., et al. 2019,
ApJ, 886, 120, doi: [10.3847/1538-4357/ab46b2](https://doi.org/10.3847/1538-4357/ab46b2)
- Skumanich, A. 1972, ApJ, 171, 565,
doi: [10.1086/151310](https://doi.org/10.1086/151310)
- Soderblom, D. R. 2010, ARA&A, 48, 581,
doi: [10.1146/annurev-astro-081309-130806](https://doi.org/10.1146/annurev-astro-081309-130806)
- Spada, F., & Lanzafame, A. C. 2020, A&A, 636,
A76, doi: [10.1051/0004-6361/201936384](https://doi.org/10.1051/0004-6361/201936384)
- Strolger, L. G., Gott, A. M., Carini, M., et al.
2014, AJ, 147, 49,
doi: [10.1088/0004-6256/147/3/49](https://doi.org/10.1088/0004-6256/147/3/49)
- Subasavage, J. P., Jao, W.-C., Henry, T. J., et al.
2017, AJ, 154, 32,
doi: [10.3847/1538-3881/aa76e0](https://doi.org/10.3847/1538-3881/aa76e0)
- Virtanen, P., Gommers, R., Oliphant, T. E., et al.
2020, Nature Methods, 17, 261,
doi: [10.1038/s41592-019-0686-2](https://doi.org/10.1038/s41592-019-0686-2)
- Yu, J., & Liu, C. 2018, MNRAS, 475, 1093,
doi: [10.1093/mnras/stx3204](https://doi.org/10.1093/mnras/stx3204)
- Zhang, S., Luo, A. L., Comte, G., et al. 2019,
ApJS, 240, 31, doi: [10.3847/1538-4365/aafb32](https://doi.org/10.3847/1538-4365/aafb32)

Table 4. Rotation-based Age Determinations for Exoplanet-Hosting M Dwarfs

Star Name	Age (Gyr)	Age err ¹	Relationship Used	Note ²
USco1621 A	0.17	0.01	mid-late	
HATS-74 A	0.18	0.01	early	
AU Mic	0.18	0.01	early	
COCONUTS-2 A	0.19	0.01	mid-late	
USco1556 A	0.24	0.01	mid-late	
K2-284	0.32	0.02	early	
TOI-620	0.33	0.02	early	
K2-104	0.34	0.02	early	
K2-240	0.42	0.02	early	
Kepler-1512	0.47	0.01	mid-late	
GJ 463	0.67	0.03	early	
Kepler-1410	0.68	0.05	early	
TOI-540	0.72	0.02	M4+	
EPIC 211822797	0.73	0.07	early	
TRAPPIST-1	0.75	0.02	M4+	
TOI-1227	0.76	0.02	M4+	
2MASS J04372171+2651014	0.77	0.02	M4+	
K2-25	0.77	0.02	M4+	
GJ 9066	0.77	0.02	M4+	
HATS-76	0.79	0.05	early	
Kepler-45	0.87	0.05	early	
K2-415	0.89	0.03	M4+	

Table 4 *continued on next page*

Table 4 (*continued*)

Star Name	Age (Gyr)	Age err ¹	Relationship Used	Note ²
GJ 338 B	0.97	0.06	early	1
Kepler-1229	1.13	0.09	early	
Kepler-1455	1.24	0.10	early	
K2-345	1.27	0.15	early	
TOI-1685	1.44	0.07	mid-late	
G1 49	1.46	0.09	early	1
Kepler-395	1.56	0.14	early	
Kepler-705	1.6	0.14	early	
TOI-1201	1.95	0.23	mid-late	
GJ 685	2.06	0.49	early	
GJ 3470	2.08	0.15	early	
K2-264	2.36	0.19	early	
TOI-3714	2.54	0.18	early	
K2-286	2.72	0.65	early	
K2-95	2.83	0.40	mid-late	
Kepler-155	2.96	0.27	early	
GJ 740	3.03	0.27	early	
GJ 514	3.05	0.31	early	
G 9-40	3.09	0.15	mid-late	
K2-332	3.14	0.16	mid-late	
GJ 96	3.16	0.32	early	
L 168-9	3.17	0.32	early	
GJ 3323	3.18	0.16	mid-late	1
HD 147379	3.25	0.65	early	

Table 4 *continued on next page*

Table 4 (*continued*)

Star Name	Age (Gyr)	Age err ¹	Relationship Used	Note ²
Kepler-1652	3.26	0.33	early	
K2-18	3.35	0.20	mid-late	
LP 714-47	3.39	0.37	early	
GJ 3293	3.43	0.21	mid-late	
HATS-71	3.44	0.21	mid-late	
LSPM J2116+0234	3.46	0.24	mid-late	
GJ 393	3.47	0.38	early	
TOI-1468	3.48	0.24	mid-late	
TOI-776	3.48	0.38	early	
HATS-75	3.53	0.39	early	
TOI-1759	3.57	0.39	early	
GJ 720 A	3.61	0.40	early	
HD 260655	3.72	0.45	early	
Kepler-560	3.73	0.30	mid-late	
G1 686	3.78	0.45	early	
TOI-700	3.85	0.31	mid-late	
Kepler-235	3.86	0.46	early	
TYC 2187-512-1	3.91	0.47	early	
GJ 9689	3.91	0.47	early	
K2-3	3.94	0.47	early	
GJ 3138	4.11	0.53	early	
GJ 1252	4.23	0.42	mid-late	
LHS 1678	4.23	0.55	mid-late	
KOI-4777	4.24	0.59	early	

Table 4 *continued on next page*

Table 4 (*continued*)

Star Name	Age (Gyr)	Age err ¹	Relationship Used	Note ²
GJ 4276	4.25	0.43	mid-late	
TOI-1235	4.31	0.60	early	
GJ 1265	4.47	0.49	mid-late	
GJ 436	4.53	0.50	mid-late	1
TOI-122	4.55	0.64	mid-late	
TOI-1695	4.57	0.69	early	
LHS 1815	4.58	0.69	early	
TOI-2136	4.68	0.56	mid-late	
GJ 536	4.78	0.72	early	
L 98-59	4.81	0.63	mid-late	
HD 180617	4.85	0.78	early	
GJ 625	4.91	0.79	early	1
TOI-674	4.99	0.85	early	
YZ Cet	5.04	0.71	mid-late	1
GJ 3512	5.22	0.73	mid-late	
Proxima Cen	5.32	0.74	mid-late	1
GJ 411	5.43	0.92	early	1
GJ 3779	5.62	0.84	mid-late	
Wolf 1061	5.62	0.84	mid-late	1
GJ 367	5.65	1.07	early	
G 264-012	5.89	0.94	mid-late	
TOI-237	6.00	1.14	mid-late	
LTT 3780	6.11	1.10	mid-late	
GJ 3929	7.21	1.51	mid-late	

Table 4 *continued on next page*

Table 4 (*continued*)

Star Name	Age (Gyr)	Age err ¹	Relationship Used	Note ²
GJ 251	7.21	1.44	mid-late	
GJ 1132	7.23	1.45	mid-late	
Ross 128	7.28	1.46	mid-late	
GJ 1214	7.4	1.48	mid-late	
GJ 1002	7.48	1.57	mid-late	
CD Cet	7.5	1.58	mid-late	
GJ 486	7.76	1.63	mid-late	
LHS 1140	7.83	1.64	mid-late	
TOI-1634	8.32	2.83	early	
GJ 1151	8.51	1.96	mid-late	
Wolf 1069	10.23	2.76	mid-late	
GJ 273	10.3	2.78	mid-late	1
GJ 3473	11.04	3.09	mid-late	
HD 238090	12.45	3.86	early	

NOTE— ¹As explained in the text, uncertainties along the younger branch (Age \lesssim 2.9 Gyr) do not account for the full scatter of rotation rates in clusters, and are therefor underestimated. Additionally, some rotation rates from the Exoplanet Archive did not have uncertainties. ² A Note = 1 indicates that the rotation rate was updated to match the value presented either elsewhere in this paper, or in the follow-up paper.